

to limit the possibilities. All $\log ft$ values are in the allowed distribution.²⁸ The $\log ft=6.8$ for the decay to the 1238 state is high enough so that positive parity cannot be ruled out. Assignments of $\frac{5}{2}$, $\frac{7}{2}$, or $\frac{9}{2}$ with negative parity are the most probable for any of this group.

The levels above 1433 keV. While our limit is $<4 \times 10^{-4}$ /decay for the 1660-keV transition, the low energy available for capture decay (~ 400 keV) still leaves the $\log ft$ value well into the allowed range; so that the present evidence cannot rule out $\frac{5}{2}$, $\frac{7}{2}$, or $\frac{9}{2}$ with negative parity for the states between 1433 and 2066 keV (the available decay energy).

ACKNOWLEDGMENTS

We wish to thank Dr. R. E. Holland for supplying the scandium metal foil and both Dr. Holland and Dr. R. D. Lawson for interesting discussions about the levels in Sc⁴⁶. We are also indebted to J. Lerner and G. Lamich for their preparation of the isotope separator source for the beta spectrometer, to A. J. Gorski for his co-operation while we were using the germanium detector in the Argonne Special Materials Division, to Dr. H. Bolotin for the use of his germanium detector and associated electronics, and to C. Batson for handling some of the data.

Polarization in the Elastic Scattering of Protons from Carbon and Nitrogen*

J. D. STEBEN† AND M. K. BRUSSEL

Department of Physics, University of Illinois, Urbana, Illinois

(Received 26 August 1965; revised manuscript received 3 February 1966)

The polarization of protons elastically scattered from nitrogen and carbon has been measured using double-scattering techniques. The polarization was determined for nitrogen at a scattering angle of $48^\circ_{e.m.}$ in the proton-energy interval 12.6 to 13.6 MeV. The polarization resulting from elastic proton scattering with nitrogen targets had a constant value of -0.60 ± 0.10 in the incident proton-energy interval 8.2 to 11.8 MeV. The polarization from carbon, however, varied markedly with energy at most scattering angles. [Example: $P(50^\circ_{lab}, 12.9 \text{ MeV}) = -0.8$, $P(50^\circ, 13.2) = -0.4$, and $P(50^\circ, 13.5) = -0.7$.] At numerous angles between 20° and 140° , polarization measurements from carbon covered the range of energies from 12.8 to 13.4 MeV. The angular distributions of polarization (and cross section) are in general quite sensitive to small changes in energy; the 12.95- and 13.25-MeV angular distributions even differ in shape significantly for $\theta > 90^\circ$. The energy-averaged (12.8- to 13.4-MeV) angular distribution for the polarization of protons scattered from carbon was compared with optical-model calculations.

I. INTRODUCTION

DESPITE the basically unsolved status of the problem of nuclear forces, various theories have been quite successful in the phenomenological description of nuclear reactions. Of these, perhaps the most striking quantitative success has been achieved with the optical model of nuclear interactions. The use of the optical model has been particularly successful in describing nucleon-nucleus elastic scattering,¹ especially from medium and heavy nuclei. It has also provided a helpful tool in understanding more complex nuclear

reactions.² There are many aspects of the nucleon-nucleus interaction, however, which the optical model is not expected to describe. Some of these (such as the detailed energy dependence of various processes) are still largely unexplained or unexplored.

While the optical model has been systematically used to analyze scattering from nuclei throughout the periodic table, from the heaviest nuclei to deuterium, there exists some question regarding its meaningful applicability to light nuclei. Despite this, a considerable amount of experimental data for proton scattering from carbon has been subjected to optical-model analyses^{3,4} with a fair degree of success.

In the present investigation, protons were elastically

* Work supported by U. S. Office of Naval Research. This paper is based on a thesis submitted (by J. D. S.) in partial fulfillment of the requirements for the Ph.D. degree in physics at the University of Illinois, Urbana, Illinois.

† Presently at Midwestern Universities Research Association, Stoughton, Wisconsin.

¹ F. G. Perey, Phys. Rev. **131**, 745 (1963); L. Rosen, J. G. Beery, A. S. Goldhaber, and E. H. Auerbach, Ann. Phys. (N. Y.) **34**, 96 (1965).

² W. Tobocman, *Theory of Direct Nuclear Reactions* (Oxford University Press, London, 1961).

³ J. S. Nodvik, C. B. Duke, and M. A. Melkanoff, Phys. Rev. **125**, 975 (1962).

⁴ L. Rosen, P. Darriulat, H. Faraggi, and A. Garin, Nucl. Phys. **33**, 458 (1962).

scattered from nitrogen and carbon. Both the angular and energy dependence of the proton polarization were measured. The energy dependence of the polarization was studied for proton energies up to 13.5 MeV with much finer energy resolution⁵ (as fine as 2%) than used previously (greater than 10%) in investigations above 10 or 11 MeV.

Specifically, we have measured the polarization of protons elastically scattered from nitrogen (99.63% N¹⁴, 0.37% N¹⁵) at 45° in the laboratory system over the region of incident proton energies between 7.7 and 11.8 MeV. For carbon (98.89% C¹², 1.11% C¹³), measurements encompassing a range of scattering energies and angles were made, with the energies in all cases lying between 12.6 and 13.6 MeV. The angular range was between 20° and 140°. An average over energy was performed to give a polarization angular distribution, $P(\theta)$, at 13.1 (12.8–13.4) MeV. Polarization angular distribution experiments had been performed previously⁶ at closely spaced energies below 11.7 and above 14 MeV.^{4,7–11}

An optical-model analysis of the $P(\theta)$ data from the present experiment was carried out, and comparisons with predictions based on other sets of data^{10,11} were made. A phase-shift analysis^{12,13} would be relevant in understanding the detailed energy dependence of the polarization, but was not performed in the present work.

This report has several purposes. It fills in the knowledge of $P(\theta)$ for carbon in an energy region not previously studied. Also, the structure in the polarization energy dependence $P(E)$ has been investigated for both carbon and nitrogen at energies corresponding to compound nucleus excitations between 14 and 18

MeV. These results imply interesting new possibilities and limitations for polarization measurements with 45° and 50° polarimeters.

II. THEORY

Two theoretical methods have been used almost exclusively in the systematic analysis of nucleon-nucleus elastic scattering in recent years. They involve (1) the use of the optical model of nuclear scattering, and (2) detailed phase-shift analyses.

The optical model provides the more direct approach of the two methods. The phase-shift methods often use optical-model phases as their starting points. This would probably be necessary at the energies of the present experiment. There are many phase shifts which contribute to the scattering process at these energies, and a unique and meaningful phase-shift analysis would be difficult to achieve with differential-scattering cross-section data, $\sigma(E)$,¹⁴ alone.¹² More precise $P(E)$ and $\sigma(E)$ data in smaller energy increments at lower energies will probably be necessary before an unambiguous phase-shift analysis can be made. At the present time, however, one can analyze the data in terms of the optical model.

Since the optical model is intended to describe direct interactions, which take place in a time commensurate with the transit time of a particle moving through the nucleus, typically 10⁻²² sec, one knows by the Heisenberg uncertainty principle that the intermediate nuclear state associated with this time definition would have an uncertainty in energy of the order of 5 MeV. Correspondingly, one would not expect that such a direct reaction approach could predict energy variations of cross sections or polarizations with much finer detail.

In the optical-model theory, the Schrödinger equation for nonrelativistic spin- $\frac{1}{2}$ particles is solved with a complex nuclear potential. In the present experiment the potential is taken as

$$V = V_{ES}(r) - V_{\rho_1}(r) - iW_{\rho_2}(r)$$

$$- \left(\frac{\hbar}{m_{\pi}c} \right)^2 \frac{1}{r} \frac{d}{dr} [\rho_1(r)] \mathbf{l} \cdot \boldsymbol{\sigma}. \quad (1)$$

The radial factors for his potential have the Woods-Saxon shape¹⁵ and the radial derivative of this shape, i.e.,

$$\rho_1(r) = \frac{1}{1 + \exp[(r-R)/a]}, \quad (2)$$

¹⁴ σ , the differential scattering cross section (differential only with respect to solid angle), is expected to be a function of both energy E and scattering angle θ .

¹⁵ M. A. Melkanoff, J. S. Nodvik, D. S. Saxon, and R. D. Woods, Phys. Rev. **106**, 793 (1957); R. D. Woods and D. S. Saxon, *ibid.* **95**, 577 (1954).

⁵ The energies of protons just before scattering vary, due to the energy spread of the incident beam, and to the finite target thickness. This range of energies is hereafter referred to as the "range of proton energies in the interaction." The energies will be given in the laboratory system. The range of proton energies in the interaction must not be confused with such things as the range of energies of the protons leaving the target.

⁶ Published or reported angular distribution data exist at the following energies (MeV): 3, 4.4, 4.66, 5.04, 6.18, 6.77, 7.21, 7.55, 7.99, 8.6, 8.66, 9.2, 10.5, 11.7, 14, 14.5, 16, 16.6, 17.7, 19.3, 19.7, 20.9, and higher energies. The gap between 11.7 and 14 MeV is certainly the largest.

⁷ S. J. Moss and W. Haerberli, Nucl. Phys. **72**, 417 (1965).

⁸ S. Yamabe, M. Kondo, S. Kato, T. Yamazaki, and J. Ruan, J. Phys. Soc. Japan **15**, 2154 (1960).

⁹ L. Drigo *et al.*, Phys. Rev. Letters **12**, 452 (1964); Yu. A. Nemilov and L. A. Pobedonostsev, Zh. Eksperim. i Teor. Fiz. **43**, 382 (1962) [English transl.: Soviet Phys.—JETP **16**, 274 (1963)]; D. Hoare, A. B. Robbins, and G. W. Greenlees, Proc. Phys. Soc. (London) **77**, 830 (1961); E. Boschitz, Nucl. Phys. **30**, 468 (1962); E. T. Boschitz, R. W. Bercaw, and J. S. Vincent, Bull. Am. Phys. Soc. **9**, 439 (1964); K. W. Brockman, Jr., Phys. Rev. **110**, 163 (1958).

¹⁰ L. Rosen and W. T. Leland, Phys. Rev. Letters **8**, 379 (1962); L. Rosen and L. Stewart, *ibid.* **10**, 246 (1963).

¹¹ L. Rosen, J. E. Brolley, Jr., and L. Stewart, Phys. Rev. **121**, 1423 (1961).

¹² G. G. Shute, D. Robson, V. R. McKenna, and A. Z. Berzits, Nucl. Phys. **37**, 535 (1962); V. R. McKenna, A. M. Baxter, and G. G. Shute, Australian J. Phys. **14**, 196 (1961).

¹³ C. W. Reich, G. C. Phillips, and J. L. Russell, Jr., Phys. Rev. **104**, 143 (1956).

and

$$\rho_2(r) = \frac{d}{dr} \left(\frac{-4b}{1 + \exp[(r-R)/b]} \right), \quad (3)$$

for the real and imaginary parts, respectively (a and b are adjustable surface parameters; r is the radial coordinate). The electrostatic interaction is taken to be of the form

$$V_{ES}(r) = \begin{cases} \frac{Ze^2}{r} & \text{for } r \geq R, \\ -\frac{Ze^2}{r} \left(3 - \frac{r^2}{R^2} \right) & \text{for } r \leq R, \end{cases} \quad (4)$$

corresponding to a sphere of constant electric charge density with a radius equal to the nuclear potential radius R . No imaginary spin-orbit potential is used (as it is usually unimportant at these energies).³ The "Thomas form" of the spin-orbit potential (apart from a sign) can be derived in the Born approximation¹⁶ (applicable at higher energies) so it seems plausible to also use this form here. The central-imaginary-potential choice is quite arbitrary except that the form used has its maximum value at the nuclear surface. The considerable experimental evidence indicates that absorption is maximum at the nuclear surface.^{3,1}

The Schrödinger equation was solved numerically by the computer program ABACUS,¹⁷ by the method of phase shifts.

Since the polarization \mathbf{P} induced by a scattering is perpendicular to the plane of scattering, one may write

$$\mathbf{P} = P\mathbf{n}, \quad \mathbf{n} = \frac{\mathbf{p} \times \mathbf{p}'}{|\mathbf{p} \times \mathbf{p}'|}, \quad (5)$$

using the Basel convention¹⁸ and letting \mathbf{p} denote the incident-proton momentum. The number of events observed for an elastic double-scattering experiment is given by

$$N = (\text{const}) \times \sigma_1(\theta_1) \sigma_2(\theta_2) [1 + \mathbf{n}_1 \cdot \mathbf{n}_2 P_1(\theta_1) P_2(\theta_2)], \quad (6)$$

where 1 and 2 denote first and second scatterings, and $\sigma(\theta)$ denotes the cross section for scattering an unpolarized beam. For two scatterings in the same plane $\mathbf{n}_1 \cdot \mathbf{n}_2$ equals +1 or -1, and N will be denoted N_b or N_f , respectively. N_f denotes two scatterings of opposite directional senses (i.e., right and left or left and right). The "f" indicates that the momentum \mathbf{p}_f'' of the

doubly scattered particle is more nearly parallel to the momentum \mathbf{p} of the incident beam ("forward" direction) than if both scatterings were of the same sense. Conversely N_b is the number of events resulting from two scatterings of the same sense (i.e., both left or both right). The corresponding proton momentum is called \mathbf{p}_b'' .¹⁹ When the second scattering is observed at the same scattering angle θ_2 to left and right, the numbers of events are then given by

$$N_i = \begin{cases} N_b \\ N_f \end{cases} = (\text{const}) \times \sigma_1(\theta_1) \sigma_2(\theta_2) \times [1 \pm P_1(\theta_1) P_2(\theta_2)], \quad (7)$$

and the counting asymmetry²⁰ is therefore the product of the polarizations, i.e.,

$$\epsilon \equiv (N_b - N_f) / (N_b + N_f) = P_1(\theta_1) P_2(\theta_2). \quad (8)$$

III. EXPERIMENTAL DETAILS

A. Apparatus and Experimental Procedure

The polarization facility used for this experiment consisted of a 25-cm-diam cylindrical scattering chamber and a special 45° polarimeter suitable for use with either solid or gaseous targets. It is described elsewhere.²¹ To obtain the carbon data, the polarimeter was used in the conventional manner (i.e., measurements were made of the polarization induced in a first scattering from carbon). To calibrate the polarimeter, and to obtain the nitrogen data, however, a beam of known polarization was produced by a fixed first scattering (i.e., the proton energy, first target²² material, and scattering angle were held fixed), and the asymmetry A was measured for the second scattering.²³

The targets used for the first scattering were 0.0006-cm.-thick Ta foil (11 mg/cm²) and self-supporting carbon foils of 7.7, 4.8, and 3.3 mg/cm² areal density. In order to narrow the energy distribution of protons scattered from these fairly thick targets, the target angle τ (the angle between the incident beam and the normal to the target) was set at $\tau = \theta/2$, θ denoting the scattering angle. Generally the angle of the first scattering was restricted to the nominal angle θ plus or minus 1.8°. However, because of multiple scattering,

¹⁹ It is convenient to call this the "back" detector. Similarly, the detector which measures N_f particles of momentum \mathbf{p}_f'' is designated the "front" or "forward" detector.

²⁰ This formula, unlike most previous formulations (which involved "L's" and "R's" explicitly) holds equally well whether the first scattering is the left or the right.

²¹ J. D. Steben and M. K. Brussel, Nucl. Instr. Methods (to be published); J. D. Steben, Ph.D. thesis, University of Illinois, 1965 (unpublished).

²² The term first (second) target will be used to denote the target from which the first (second) scattering occurs.

²³ This term "asymmetry," A , is misleading if the incident beam is less than 100% polarized (and it usually is). What we will denote by asymmetry (symbol " ϵ ") in the remainder of this report is, instead, the ordinary scattering asymmetry [see Eq. (9)], which is equal to $P_1 A$ or $P_1 P_2$ rather than A or P_2 .

¹⁶ L. Wolfenstein, Ann. Rev. Nucl. Sci. **6**, 43 (1956). W. B. Riesenfeld and K. M. Watson, Phys. Rev. **102**, 1157 (1956).

¹⁷ E. H. Auerbach, N. C. Francis, D. T. Goldman, and R. C. Lubitz, ABACUS-1; Knolls Atomic Power Laboratory Report No. KAPL-3020, 1964 (unpublished); E. H. Auerbach, ABACUS-2; Brookhaven National Laboratory Report No. BNL 6562, 1962 (unpublished).

¹⁸ *Proceedings of the International Symposium on Polarization Phenomena of Nucleons, Basel, 1960*, edited by P. Huber and K. P. Meyer (Birkhauser Verlag, Basel and Stuttgart, 1961); Helv. Phys. Acta Suppl. **6**, 436 (1961).

larger angular ranges (up to $\pm 3^\circ$) resulted when a thick energy-degrading absorber was used between targets. A 7.5-mg/cm² carbon foil (in vacuum) and N_2 at a pressure of 0.8 to 1.2 atm were used as targets for the second scattering. The angle of the second scattering, θ_2 was restricted to $45^\circ \pm (6^\circ \text{ or } 8^\circ)$. For the targets used, the polarimeter has a proton energy resolution of between 3% and 4%.²¹

Several types of detectors were used in the course of this experiment. The doubly scattered protons passed through gas proportional counters 2 in. thick with $\frac{7}{8}$ in. apertures before entering the "E detectors." The proportional counters were used to select doubly scattered protons and to reject undesired events caused by neutrons and gamma rays. The proportional counters contained about 0.6 atm of argon plus 0.06 atm of CO₂. Their windows were made of 0.003-cm-thick dural²⁴ and 0.005-cm-thick Ni.

The "E detectors" were 0.16 cm-thick NaI(Tl) scintillators (3.2-cm-diam masked down to 2.2-cm) and 0.32-mm-(320- μ) thick 1.9-cm-diam Si surface-barrier detectors. The Si detectors were used when the detected protons had energies of 6 MeV or less, so that the detectors had a thickness slightly greater than that necessary to stop the protons. Slow (2 μ sec) coincidences were required between the dE/dx and E detectors, thereby eliminating the neutron and gamma-ray background.

Calculations of the effects of finite geometry [deviations from Eq. (8)] were carried out²¹ to second order in various parameters [involving Taylor series expansions of $\sigma(\theta)$ and $P(\theta)$] and the resulting expressions determine ϵ to an accuracy of 0.002. (The dimensional factors most immediately affecting the attainable accuracy in ϵ were the position of the collimator defining the second target, the angle τ between the beam and the normal to the first target, and the width of the collimators for the incoming beam.) For the present experiment, however, the spatial structure of the beam caused the major uncertainty, so it was sufficient to modify Eq. (8) as follows:

$$\epsilon \equiv (N_b - N_f)/(N_b + N_f), \quad P_1 P_2 = \epsilon - \epsilon_0, \quad (9)$$

where ϵ_0 is the asymmetry produced due to geometrical effects when P_1 and/or P_2 is zero.

Proton scattering from Ta targets, particularly at 20° where the cross section is large, was used to check geometrical asymmetries ϵ_0 (since the scattered protons are unpolarized) and data reproducibility.²⁵ These runs, generally of $\geq 10\,000$ events in the elastic peaks, were taken periodically throughout the experiment. The standard deviation in the measurements of the geometric asymmetries, after a correction for a "beam asymmetry" was applied, was approximately 0.02 for the

²⁴ Duraluminum, or 17S alloy, composition Mg $\frac{1}{2}\%$, Mn $\frac{1}{2}\%$, Cu 4%, Al 95%.

²⁵ About 40 of these geometric asymmetry runs were analyzed statistically with a short computer program.

largest collimating apertures used. Measurements with finer collimation were consistent within 0.015. These included 180° rotations of the polarimeter about its axis, and comparison between measured and calculated angular distributions of geometrical asymmetries.

The energy of the proton beam was monitored often during the experiment. Surface-barrier (Au-Si) solid-state detectors were used for this purpose. The energy monitoring systems were calibrated with the use of natural alpha-particle sources. In order to extend the effective maximum energy which the 600- to 700- μ -depleted thick Si detectors could measure, aluminum energy absorbers of known thickness were employed. Protons of energy 8 to $9\frac{1}{2}$ MeV were stopped in the sensitive region of the detector whether or not the absorber was used. By comparing the pulse heights obtained for these protons with and without Al absorbers placed before the detectors, we observed agreement with Bichsel's range energy data²⁶ to within 1%.

In addition to the energy, other quantities monitored during the course of the experiment were the "beam asymmetry," the coincidence efficiency, and the total yield,

$$(N_b + N_f)/Q \sec \tau,$$

where Q denotes integrated beam current. The "beam asymmetry" was measured by inserting a cutaway target thick enough (1.6-mm-thick C or 0.8-mm-thick Ni) to stop the beam arriving on one side of the target rotation axis. The beam to the target was measured, as well as the beam which missed the target and entered the Faraday cup. The coincidence efficiency, the fraction of the protons which were counted, was maintained between 0.992 and 0.997.

The first target was rotated 180° in the middle of each run. Both the first half and the complete run were printed out, and their asymmetries and yields were compared. This procedure provided a crude check of the uniformity of the first target. It also afforded partial insurance against loss or distortion of the data due to possible faulty operation of the apparatus or cyclotron.

Many other checks and calibrations were carried out when the cyclotron was not operating. The most important of these were the following: 1. The uniformity of the carbon target used for the second scattering was measured by the use of a "foil-thickness calibrator." In this instrument the target was moved between a Pb²¹² source and a well collimated solid-state detector. The resultant α -particle energy loss in the target was observed as a function of target position. 2. The alignment of the 45° polarimeter was checked for a number of scattering angles, at various times.

Various aluminum foils were used between targets so as to regulate the energy of protons arriving at the

²⁶ Hans Bichsel, Phys. Rev. 112, 1089 (1958).

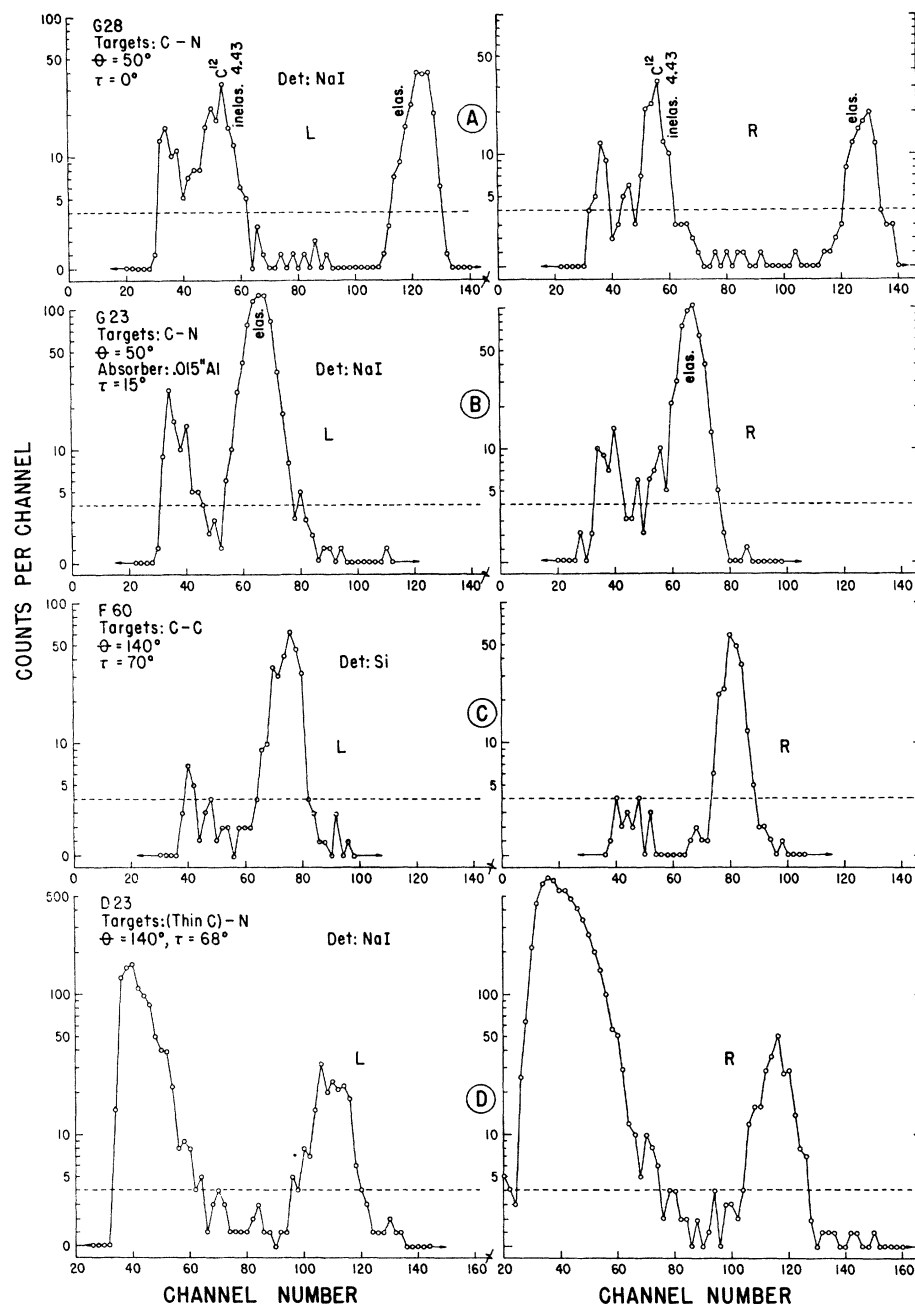


FIG. 1. Representative spectra. Part (A) displays the beneficial effect of reducing the N_2 pressure from 1.2 to 0.8 atm. As the protons are higher in energy, background is reduced and the inelastic $C^{12}(p,p^*)C^{12*}$ (4.43-MeV) peak is resolved from the background. Part (B) displays the resolution of the elastic peak from the background when a thick absorber is used between targets (with the normal N_2 pressure of 1.2 atm). Parts (C) and (D) are spectra taken at 140° where the cross section is very small and the problem of background is most serious. They also illustrate a comparison between Si and NaI detector spectra (with and without an absorber, respectively).

second target. This method of energy regulation was used during two types of measurements.

In one instance we wanted to maintain a fixed first-scattering polarization (the first target being carbon). This was done by using a fixed incident beam energy, 13.4 (8.6) MeV, and observing the scattering at a fixed angle, 50° (70°). The absorbers were then used to measure the energy dependence $P_2(E_2)$ of the polarization of the second target, nitrogen (carbon), in the energy range from 7.7–11.9 MeV (5.4–6.8 MeV).

In the other instance, when the carbon-analyzed carbon data were being taken, the absorber had to be carefully chosen to keep E_2 at 6.0 ± 0.3 MeV. If this energy were increased, a loss of analyzing power would result. Any lower energy E_2 would cause a problem of background. For the carbon angular distributions analyzed with nitrogen targets, however, no inter-target absorber was necessary, since the nitrogen polarization is large and relatively insensitive to energy in the range of energies E_2 (8.5–11.8 MeV) that occurred without an absorber.

B. Data Analysis

To obtain polarization information from the data, the following basic steps were taken: (1) Various corrections were employed to determine $\epsilon - \epsilon_0$, or $P_1 P_2$. (2) The average energies E_1 and E_2 and the energy distributions of the first and second scatterings were accurately determined. (3) Individual polarizations were calculated from the corrected asymmetries, i.e., from the products of polarizations $P_1(\theta, E_1) P_2(45^\circ_{\text{lab}}, E_2)$. These three steps will be discussed in order.

1. Determination of Corrected Asymmetries

While the coincidence requirements removed more than 99% of the background events from the spectrum, a few accidental coincidences still occurred which permitted neutrons or γ rays in the energy range of the elastically double-scattered protons to be counted. Background subtraction was applied to all runs for the sake of consistency, although the "peak-to-valley" ratios were in general greater than 40 [as in Fig. 1(A)], and background was usually unimportant.

The next important correction was to subtract ϵ_0 , the geometrical asymmetry previously mentioned (including beam asymmetry) from ϵ . Since ϵ_0 is a function of the cross sections, appropriate experimental data were used for carbon²⁷ and nitrogen.¹¹ (The tantalum cross section was Coulombic at the angles and energies used.)

The uncertainties in $(\epsilon - \epsilon_0)$ have been calculated by assuming that effects due to background, misalignment, and finite geometry are uncorrelated and combining them quadratically. The uncertainty in background subtraction was conservatively taken as $\frac{1}{3}$ of the background subtracted, for each spectrum. The uncertainty that existed in the alignment of the polarimeter was negligible. The machining tolerances (± 0.001 in.) in the polarimeter and the collimating system were checked, and the sum of these uncertainties (the systematic error) contributes less than 0.002 to the uncertainty in $(\epsilon - \epsilon_0)$. The dominant sources of uncertainty were "beam asymmetry" and counting statistics.

2. Energy Measurement

The determination of the energy distributions, $e_1(E)$ and $e_2(E)$ of protons undergoing interactions in both targets (and also the corresponding energy distribution e_0 for the incident proton beam) turned out to be a very important part of this experiment. A determination of the average energies E_1 , E_2 , and E_0 , respectively, was made using a computer program. The information furnished to this program was the elastic peak channel (the channel with the most counts) from the energy monitor spectra, the channel-versus-energy calibration, the range-versus-energy relations for aluminum and air, the specific ionization curves for Mylar and carbon,

and the relevant kinematical equations. The accuracy of the knowledge of average (relative) energies so obtained varied from $\pm(30$ to $80)$ keV, depending on the amount of energy-monitor information available. The lower limit corresponds to runs in which six energy-monitor spectra were taken. The absolute energy uncertainty was estimated to be ± 60 keV.

As discussed in Sec. I, the protons which underwent scattering in the targets had a range of energies for each of the data points. In general, the energy spread of the beam (about 150 keV at 13 MeV), combined with the first target thickness of 175–300 keV, produced a total energy spread of 250–330 keV in the first scattering. The energy spread of protons in the second scattering [in 1.2 (0.8) atm N_2] would be approximately 280 (220) keV if a monoenergetic beam of 11.0 MeV were incident on that target. However, when the 280–(220-) keV energy spread is involuted with the energy spread of the once-scattered beam, the range of proton energies in the second target interaction is increased to 300 (260) keV. An upper limit to the energy spread of the proton beam at any given point in the second target was observed in the proton spectrum of the center (energy-monitor) detector.

In general, for the carbon $P(\theta)$ measurements near 13 MeV, the energy spread [i.e., width of $e_1(E)$] was 2 to 3% of the total energy. For the nitrogen (second target) measurements it was $2\frac{1}{2}$ to 5%. When carbon was used as a second target and a thick aluminum absorber was placed between targets to reduce the

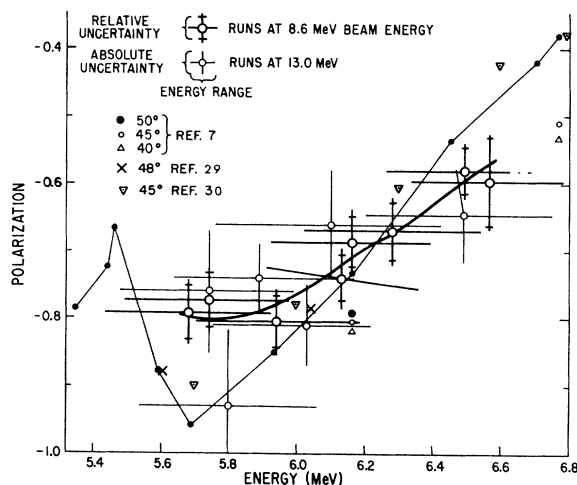


FIG. 2. Calibration of the carbon polarization analyzer. [Graph of $P(45^\circ_{\text{lab}})$ versus energy for scattering from carbon second targets.] Vertical lines denote the total uncertainty. The statistical standard deviation in the asymmetry ϵ causes an uncertainty indicated by the region between the cross bars. Horizontal lines denote the range of proton energies in the interaction (a phrase carefully defined in footnote 5). This convention will be followed whenever the horizontal axis designates energy. The uncertainties (not shown) in the median energies for the data points are all ± 40 keV. A heavy line has been drawn through our calibration data, and it denotes the $P_2(\bar{E}_2)$ which was used in analyzing the 13-MeV data.

²⁷ Yukio Nagahara, J. Phys. Soc. Japan 16, 133 (1961).

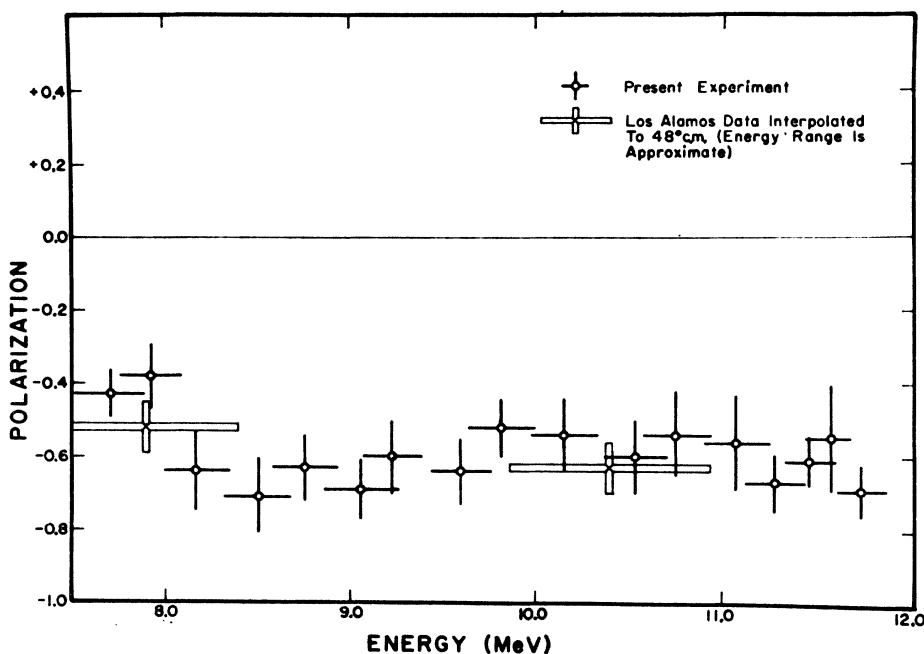


FIG. 3. Polarization of protons elastically scattered from nitrogen at 48° c.m. (45° lab). As in Fig. 2, horizontal full lines denote spread rather than uncertainty in energy. The uncertainty in the median energy of each datum is ± 50 keV. The "Los Alamos data" are derived from Refs. 11 and 28.

proton energy (from about 12 MeV) to 6 MeV, however, the resulting energy spread was as large as 10 to 12%.

3. Determination of Polarizations from Corrected Asymmetries

Once the set of products of polarizations of all the runs (about 140 in these experiments) is known, one may obtain the individual polarizations. Previously reported data^{7,28} shown in Table I, were used to calibrate the polarimeter. In particular, one finds that $P(C^{12}, 70^{\circ}$ lab, 8.0–8.6 MeV) = 0.95 ± 0.04 . We used this value as P_1 to calibrate a carbon second target (i.e., to find $P_2(C^{12}, 45^{\circ}$ lab, \bar{E}_2) for energies E_2 between 5.4 and 6.8 MeV). The "bar" on the E_2 indicates that a sizable energy range (500 keV) is being averaged over.

The polarization-versus-energy calibration for this second target (7.5 mg/cm² C) is shown in Fig. 2. Also shown are polarization excitation function data from other experiments,^{7,29,30} generally taken with thinner

targets, at angles between 40° lab and 50° lab. Small discrepancies between our data and the latter may be attributed to differing energy spreads for measurements centered about the same quoted energies. Our C^{12} polarimeter calibration $P_2(45^{\circ}, \bar{E}_2)$ (the heavy line through our points in Fig. 2) was then used to analyze many of the 13-MeV carbon data.

A similar polarimeter calibration, $P_2(45^{\circ}, E_2)$ for N^{14} between 8 and 12 MeV (shown in Fig. 3), was used to analyze the rest of the 13-MeV carbon measurements.

The carbon angular-distribution data for the various proton energy intervals were deduced from the excitation function data (of Sec. IV, Figs. 4–5). Two methods were used for this calculation.²¹ The results of the two methods agreed within 0.06 in all cases and within 0.03 for the cases involving an average over the 12.8- to 13.4-MeV energy interval.

IV. RESULTS AND DISCUSSIONS

In the following, the results are presented and discussed in three sections: The 48° nitrogen-polarization excitation-function data constitute part A. The 12.6- to 13.6-MeV carbon data constitute parts B and C. The actual data points are shown in B as excitation functions. The angular distributions are shown in C and were computed from these excitation functions.

A. Nitrogen Data

The energy dependence of the polarization of protons scattered elastically at 48° c.m. (45° lab) from gaseous nitrogen (99.63% N^{14} , 0.37% N^{15}) has been measured between 7.6 and 11.8 MeV. The angular range of the scattering, defined by the geometry of the 45° polarim-

TABLE I. Available carbon data used for calibration purposes.

Purpose	Average proton energy E (MeV)	Approx. energy range δE (MeV)	Ref.	Polarization $P(74.5^{\circ}$ c.m.)
Calibration runs for carbon second target	7.99	0.165	7	$+1.03 \pm 0.05$
polarization analyzer	8.66	0.155	7	$+0.92 \pm 0.13$
	8.6	1.0	28	$+0.96 \pm 0.04$

²⁸ L. Rosen, J. E. Brolley, Jr., M. L. Gursky, and L. Stewart, Phys. Rev. **124**, 199 (1961).

²⁹ J. E. Evans, Helv. Phys. Acta Suppl. **6**, 239 (1961); J. E. Evans, Nucl. Phys. **27**, 41 (1961).

³⁰ R. E. Warner and W. P. Alford, Phys. Rev. **114**, 1338 (1959).

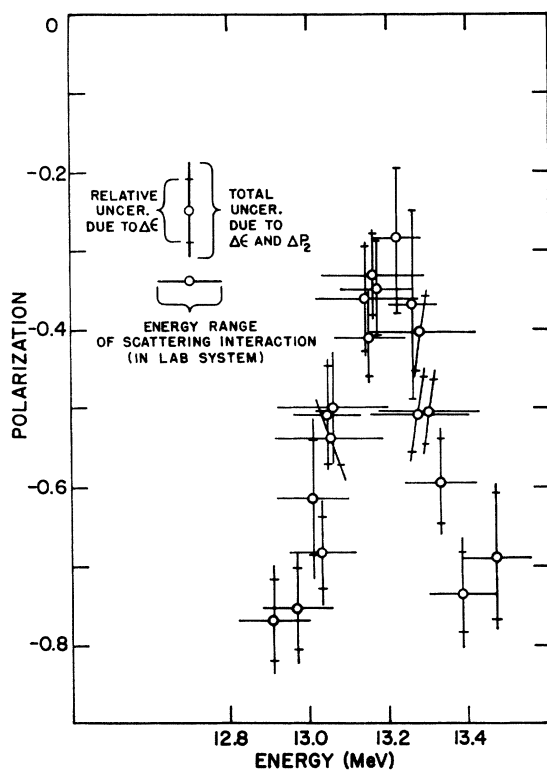


FIG. 4. Polarization of protons elastically scattered from carbon at 53.7° c.m. (50° lab). The relative uncertainty due to $\Delta\epsilon$ is the uncertainty which would result if P_2 were known exactly.

eter, extended from about 37° lab to 53° lab. The data are shown in Fig. 3. The symbols shown on this graph are data in the present experiment, except for two points based on measurements of Rosen *et al.* (see Table I)^{11,28} taken with thick targets. Our data when averaged over energy agree fairly well with Rosen's.

The most impressive feature of the data is the plateau which extends from 8.2 to 11.8 MeV. The polarization appears to be quite uniform with a value of -0.60 ± 0.08 throughout the entire interval. The polarization curve drops off substantially for proton energies less than 8.2 MeV.

The main factors limiting the accuracy of the nitrogen data are the uncertainty in the knowledge of the incident beam energy and the fact that the polarizing power of the first target was energy-dependent.

Since a polarization of -0.60 fits the data above 8.2 MeV with no sizable fluctuations (fluctuations probably are less than ± 0.08), the nitrogen second target was used in this experiment as a polarization analyzer for protons scattered from carbon. Since $P_2 = -0.60 \pm 0.08$ could be used throughout the energy interval 8.2 to 11.8 MeV, it was unnecessary to measure accurately and compute the energy E_2 of the second scattering in each individual case.

Nitrogen would also be a useful analyzer for polarizations produced in inelastic scattering ($Q \geq -3.0$ MeV)

or (X,p) reactions (X =anything), since the $N^{14}(p,p')-N^{14*}$ (2.31-MeV) cross section is negligible^{21,31} and the next excited state is at 3.95 MeV.

B. Carbon Data—Excitation Functions

A large number of carbon polarization measurements in the 12.6- to 13.6-MeV energy range were made, some with carbon and the rest with nitrogen second targets as the polarization analyzers. The analyzing powers for the second scatterings, at 45° , were the polarizations shown in Figs. 2 and 3.

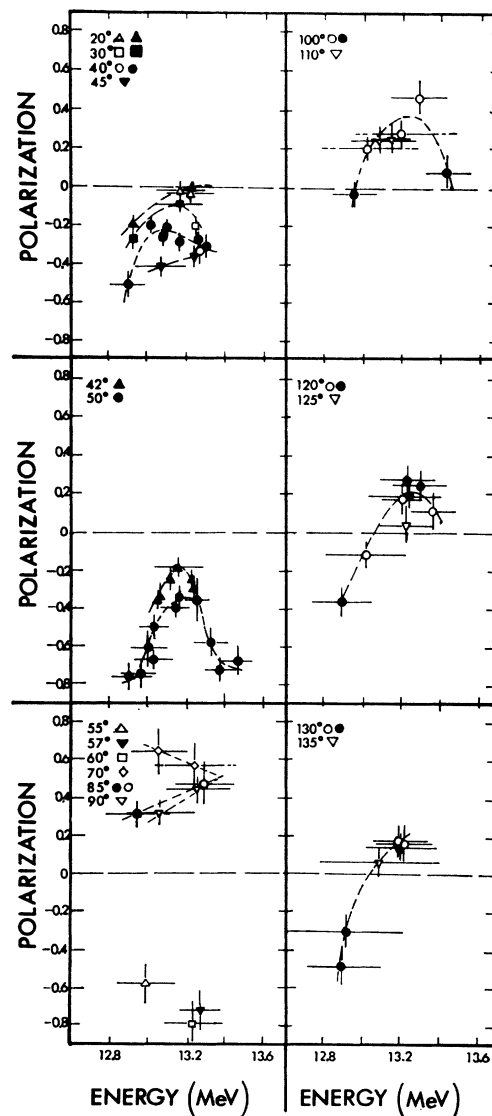


FIG. 5. Excitation functions of the polarization on protons scattered at various angles from carbon. Angles shown are in laboratory system. The curves are drawn merely to guide the eye through data points taken at the same angle.

³¹ P. F. Donovan, J. F. Mollenauer, and E. K. Warburton, *Phys. Rev.* **133**, B113 (1964).

While the original intention was to take an angular distribution of the polarization at one energy, the polarization fluctuated with the 100- to 200-keV changes in beam energy arising from cyclotron tuning. The data could therefore not be consistently evaluated without knowing the energy more accurately. We could have used very thick targets to average out this effect as Sanada did,³² but felt there was more to learn by measuring the energy accurately and studying this energy dependence of the polarization.

As the scattering angle could be set with more precision than the energy, the data naturally fell into groups comprising excitation functions at various angles. These excitation functions were then extended by raising and lowering the nominal cyclotron energy so that the polarization in the proton energy range between 12.8 and 13.4 MeV was ascertained at most angles.

The excitation functions of the carbon polarization at various angles are shown in Figs. 4 and 5. An extensive series of measurements was made at 50° to test the reproducibility of the data (see Fig. 4), and hence the accuracy and reliability of the energy monitoring system. In the process, the 50° data were retaken with thinner targets (120 to 170 keV thick to protons) to observe the finest structure resolvable with a proton beam of 150-keV energy width. Only the energy spread due to target thickness is shown in Figs. 4 and 5, but in almost all cases the target thickness was 70% to 90% of the range of proton energies in the interaction.⁵

A large variation of the polarization at 50°_{lab} was found to occur for an energy variation of only 300 keV. The polarization fluctuates from about -0.80 to -0.40 and back to -0.70 as the energy varies from 12.9 to 13.5 MeV. The corresponding cross section at 50° is almost constant in this energy interval.²⁷ Similar polarization effects turned up at other angles, and it may be seen from Fig. 5 that the data, almost independently of the scattering angle (except perhaps between 55° and 90°), show an algebraic maximum of the polarization near 13.15 MeV. The polarization typically varies as much as 0.40 or 0.50 within a 600-keV energy range.

As mentioned in Sec. II, such structure cannot be predicted from the simple optical model (parameters not functions of energy) or a direct-reaction mechanism. Therefore the scattering process is more complicated and it is thought that the compound nucleus N¹³ (13-MeV protons produce a 13.75-MeV excitation of N¹³) is involved. Ericson³³ has been quoted as suggesting that a relatively small compound nuclear part of the interaction could exert sizable effects on the polarization, and it can furthermore be questioned whether the

compound nuclear part is small at this excitation. Experimentally, Evans *et al.*³⁴ found an effect similar to ours in the C¹²(*d,p*) polarization where 6-MeV deuterons give a 14.3-MeV excitation in N¹⁴.

It is worth noting that 8.5-MeV protons on N¹⁴ give a compound nucleus excitation 1.0 MeV higher than do 13-MeV protons on C¹², and that at any given excitation (above a few MeV) O¹⁵ appears to have a somewhat greater density of states than N¹³. Consequently, it is not surprising that the energy dependence of the polarization is more severe for C¹² than for N¹⁴.

In Fig. 5 the carbon data taken with a nitrogen second target are shown by open polygons, whereas the carbon-analyzed carbon data points are shown by solid polygons. The C- and N-analyzed data can be seen to agree reasonably well, indicating that no extraneous or unexpected effects were being introduced by having a thick absorber between targets to slow the protons to 6 MeV during the carbon-analyzed runs.³⁵

The observed energy dependence of the polarization is about as complex as the present instrumentation could hope to resolve. Finer structure may exist. At large scattering angles especially, where Nagahara's cross-section data show an energy dependence as complex as that which we observed for the polarization, finer structure is to be expected. The $\sigma(E)$ cross-section structure, at 133°_{lab}, which we were able to observe in the shape of an elastic scattering peak when protons were reflected from a thick target, gave confidence that our energy determinations and Nagahara's agree within about 60 keV.

C. Carbon Angular Distributions

By performing a cross-section-weighted average of $P(\theta, E)$ over energy, we have obtained angular distributions which would result from the use of targets having thicknesses of 300 and 600 keV. This has been done for several energy intervals, and the angular distributions obtained have been plotted in Fig. 6. For those data averaged over the 600-keV energy interval, effects due to non-direct-reaction processes (compound-nucleus effects, etc.) are minimized, and the optical model in its present form is most applicable.

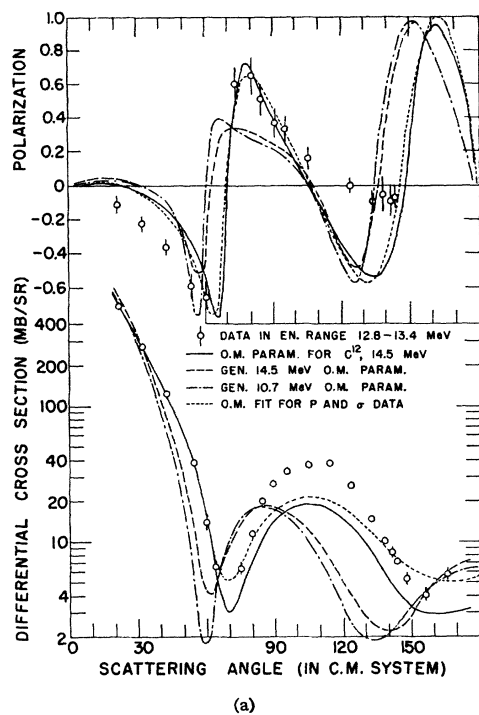
In Fig. 7 our angular distribution averaged over the 12.8- to 13.4-MeV energy interval is compared with earlier polarization measurements at higher and lower energies.^{8,10,11} One can see from Fig. 6 (b) that data with good energy resolution (300 keV) show much more variation over a small interval, 12.8-13.4 MeV, than data with poor resolution (0.6 to 2.0 MeV) show over the large interval 11-15 MeV displayed in Fig. 7.

³⁴ J. E. Evans, J. A. Kuehner, and E. Almquist, *Phys. Rev.* **131**, 1632 (1963).

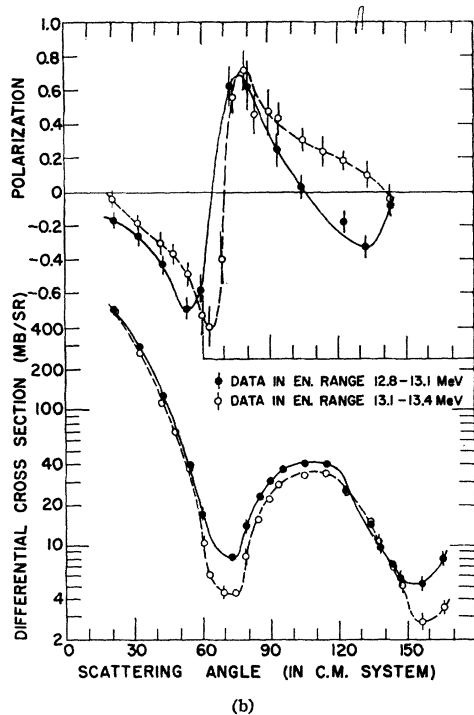
³⁵ Multiple scattering in the thick energy absorber widens the distribution of angles θ_2 in the second scattering. The effect of this on the polarization analyzing power P_2 is thought to be quite minor ($\leq 2\%$), since $P_2(\theta_2)$ varies rather slowly with respect to θ_2 near 40° for proton energies around 6 MeV.

³² J. Sanada, *Helv. Phys. Acta. Suppl.* **6**, 249 (1961).

³³ T. Ericson, in *Proceedings of the International Conference on Nuclear Structure, Kingston*, edited by D. A. Bromley and E. W. Vogt (University of Toronto Press, Toronto, 1960); R. W. Bercaw and F. B. Shull, *Phys. Rev.* **133**, B632 (1964).



(a)



(b)

FIG. 6. $P(\theta)$ and $\sigma(\theta)$ for $C^{12}(p,p)$. (a) The data shown cover the 12.8- to 13.4-MeV proton energy interval. The optical model predictions based on analyses of earlier data (Table II) are made for a proton energy of 13.1 MeV. The dotted curve is an optical-model fit to the present data and the cross-section data shown. The cross-section points are calculated from data of Nagahara (Ref. 27) by appropriate averages over energy for this and the following graph. (b) $P(\theta)$ and $\sigma(\theta)$ in lower and upper energy intervals investigated (12.8-13.1 MeV and 13.1-13.4 MeV). The curves are drawn merely to guide the eye.

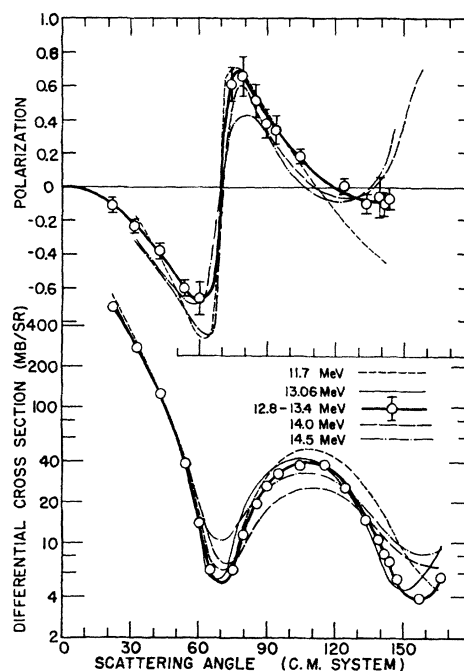


FIG. 7. Angular distribution of the polarization and differential cross section for protons elastically scattered from carbon between 11 and 15 MeV. Cross-section data are from Nagahara (Ref. 27). His angular distributions at 11.51, 13.06, 13.92, and 14.36 MeV are shown by the light curves. The heavy curve is an average of his data between 12.8 and 13.4 MeV. Polarization data are from Yamabe *et al.* (Ref. 8) at 14 MeV, Rosen *et al.* (Refs. 10 and 11) at 11.7 and 14.5 MeV, and the present experiment. Smooth curves have been drawn through all data, and to avoid confusion, the only data points and energy range shown explicitly are those from the present investigation. Energy spreads of the other polarization data are typically 1 MeV or more, and uncertainties in P are generally around 0.06.

Optical-model analyses have been performed by Beery³⁶ using the ABACUS optical-model code,¹⁷ and the predictions for the 12.8-13.4-MeV range are shown in Fig. 6 (a) along with the experimental data. Predictions based on parameters from other data^{10,11,36} and a best fit to our data (varying V , W , V_s , a , b) are shown. The corresponding optical-model parameters are shown in Table II, as they apply to Eqs. (1) to (3). The curves obtained from Rosen's parameters averaged over A for $A \geq 40$ (sets 2 and 3 in Table II) give wrong angles for the extrema and bear little relation to the ($A=12$) data. As expected, the variational fit to our $P(\theta)$ and Nagahara's $\sigma(\theta)$ data gives the closest agreement, although the parameters obtained from fitting the 14.5-MeV carbon data work almost as well. In both cases, the $P(\theta)$ curves deviate badly from the experimental points only at angles greater than 110° . The fits to carbon data (sets 1 and 4, and other fits, not shown, to P and σ separately) indicate a thin nuclear surface (which might be expected for C^{12} which is strongly bound) and indicate absorption which has a narrow maximum at the

³⁶ J. G. Beery (private communication).

TABLE II. Optical-model parameters used or obtained in the data analysis.

Values of fixed parameters: $R=r_0A^{1/3}$, $r_0=1.25$ F					
Values of parameters which were varied:					
	V	W	V_s	a	b
1. Parameters from best fit to previous 14.5-MeV proton data for carbon ($A=12$)	48.86	9.54	5.53	0.449	0.382
2. Parameters from best fit to previous 14.5-MeV proton data for $A>40$	49.00	7.50	5.50	0.650	0.700
3. Parameters from best fit to previous 10.7-MeV proton data for $A>40$	51.75	8.08	5.93	0.630	0.740
4. Search to fit P and σ of present investigation	51.13	8.92	6.06	0.458	0.325

nuclear surface. (The diffuseness parameter b is especially small.)

All of the theoretical curves predict a first maximum in $\sigma(\theta)$ which is only 50% to 70% of the observed value, and a shape for the $P(\theta)$ curve which does not too accurately fit the data at angles less than 50° . Also, there exists a second minimum in $\sigma(\theta)$ at 13 MeV (Fig. 7), something which is absent for carbon data in most of the 10- to 15-MeV range.²⁷ The combination of this second minimum and the large first maximum in $\sigma(\theta)$ leads one to think that some kind of resonance is involved and that perhaps a state or group of states of the N^{13} compound nucleus is being strongly excited. At an N^{13} excitation of 13.9 MeV, though, a simple process seems improbable, and a detailed phase-shift analysis, probably requiring a more precise excitation-function measurement of the carbon cross sections above 11.5 MeV, would be required before one could reach meaningful conclusions.

V. SUMMARY AND CONCLUSIONS

The angular distribution of the 13.1-MeV (12.8- to 13.4-MeV) energy-averaged carbon polarization lies mainly between the similar distributions at 11.7 and 14.5 MeV. The optical model calculations fit the data only qualitatively.

The existence of energy-dependent fluctuations of up to 50% in the polarization of these elastically scattered protons has been established. The polarization has been measured between approximately 12.8 and 13.5 MeV with an energy resolution of about 200 keV. The observed fluctuations lend support to the prediction of Ericson and others³³ that the presence of relatively weak compound nucleus effects would strongly influence the proton-nucleus interaction in this energy range (which

in the present case is a N^{13} excitation of about 14 MeV, where one would expect several levels to overlap).

That the nitrogen polarization data above 8.2 MeV are relatively independent of energy is consistent with the fact that the compound-nucleus excitation (14.5–18 MeV in O^{16}) is higher than in the case of N^{13} .

On a practical basis, this experiment has shown nitrogen to be a useful polarization analyzer^{37,38} (with a polarization of -0.60 ± 0.10) for 45° polarimeters throughout the 8.2- to 11.8-MeV range.

One can conclude that nitrogen is preferable to carbon in the region around 12 MeV, especially if one wants to use a thin target and resolve individual proton groups separated in energy by less than 1 MeV. This might be desirable in an experiment to examine protons from deuteron stripping with nuclei in the $A=40$ to 90 range, where more than one final state is of interest. Conversely, our experiment indicates that the energy must be known accurately in experiments using thin carbon targets (less than perhaps 15 mg/cm²) as a polarizer or analyzer in the 12- to 14-MeV proton energy range. An experiment would be desirable to extend the carbon excitation functions throughout the energy range from 12 to 15 MeV. Possibly this could be done with finer energy resolution than was here feasible.

An experiment would certainly also be desirable to calibrate a nitrogen 45° polarimeter above 12 MeV.

ACKNOWLEDGMENTS

The authors are pleased to have an opportunity to thank many people who have rendered to them assistance in this work: Dr. F. W. Bingham, for valuable advice and assistance in the computer programming and data taking; Dr. R. L. Burman, for helpful advice and for the design and construction of much of the polarization apparatus; Van Bluemel and David Rundquist, for a great deal of help in taking the data; Dr. J. C. Hafele, for helpful discussions regarding electronics; Professor J. S. Allen, for helpful advice and encouragement; Dr. J. Beery and Dr. L. Rosen of Los Alamos Scientific Laboratory, for optical-model calculations.

³⁷ The upper energy limitation to the useful range is not known, but is at least above 11.8 MeV. Nitrogen is considerably better than the only other target, helium, which has been shown capable of use at 45° in the 8- to 12-MeV energy range. The possible energy resolution is 3 to 4 times better with nitrogen than with helium, the scattered protons are much higher in energy (both effects due to kinematics), and the polarization is slightly larger.

³⁸ Note added in proof. Nitrogen data in Ref. 1 (Rosen *et al.*) at 14.5 MeV indicate roughly 60% polarization analyzing power also at that energy. R. I. Brown has recently obtained data similar to Fig. 3 in the energy range 5–10 MeV. His results seem to be consistent with ours in the region of overlap, except perhaps at 8.3 MeV (where he found a larger polarization maximum consistent with his slightly better energy resolution).